Electronic structures of Mo pyrochlore: $R_2Mo_2O_7$ (R=Nd, Sm)

J.-S. Kang,[1] Y. Moritomo,[2] Sh. Xu,[3] C. G. Olson,[4] J. H. Park,[5] S. K. Kwon,[5] and B. I. Min[5]
[1]*Department of Physics, The Catholic University of Korea, Puchon 420-743, Korea*
[2]*CIRSE, Nagoya University, Nagoya 464-8601, Japan*
[3]*Department of Crystalline Materials Science, Nagoya University, Nagoya 464-8603, Japan*
[4]*Ames Laboratory, Iowa State University, Ames, Iowa 50011*
[5] *Department of Physics, Pohang University of Science and Technology, Pohang 790-784, Korea*
(Received 28 December 2001; revised manuscript received 25 March 2002; published 6 June 2002)

The electronic structures of Mo pyrochlore systems of $R_2Mo_2O_7$ (R=Nd, Sm) have been investigated using photoemission spectroscopy (PES). The electronic states near E_F have mainly Mo $4d$ character. The R $4f$ states are located well below the Fermi level and the valence states of *bulk* Nd and Sm ions are very close to 3+. The local spin density approximation (LSDA) and LSDA+U+spin-orbit (SO) band calculations incorporating the effects of the on-site Coulomb correlation U and the SO interaction of Nd $4f$ electrons show the large hybridization between the Mo $4d$ and O $2p$ orbitals and the magnetic moment of $\sim 1.0\mu_B$ per Mo atom. The qualitative features of the measured valence-band PES spectra of $Nd_2Mo_2O_7$ agree well with the LSDA+U+SO band structure calculation. The origin of the stable ferromagnetic phase in $Nd_2Mo_2O_7$ has been discussed based on the nearly half-metallic electronic structure.

DOI: 10.1103/PhysRevB.65.224422 PACS number(s): 79.60.−i, 75.70.Pa, 71.30.+h

I. INTRODUCTION

Most metallic oxides that exhibit interesting correlations between magnetism and metallic conductivity contain $3d$ transition-metal (TM) elements.[1] Typical examples are the perovskite manganites $R_{1-x}A_xMnO_3$ (R=rare earth, A=divalent cation) that show the colossal magnetoresistance (MR) phenomenon. In these systems, the double exchange (DE) between mixed-valent Mn^{3+} and Mn^{4+} ions through oxygen ions is considered to give rise to metallic conductivity and concomitant ferromagnetism (FM). Recently a correlation between FM and metallic conductivity has also been observed in the $4d$ TM oxides, such as A_2FeMoO_6 double-perovskite oxides (A=Sr, Ba) and $R_2Mo_2O_7$ pyrochlore oxides. A_2FeMoO_6-type double perovskites show room-temperature MR with very high magnetic transition temperatures T_C,[2] while $R_2Mo_2O_7$ pyrochlores show a phase transition from the spin-glass insulating state to the FM metallic state.[3,4] The question arises whether the essential physics of ferromagnetic $4d$ TM oxides is similar to that of $3d$ $RAMO$ manganites.

The pyrochlore $A_2B_2O_7$ system crystallizes in a face-centered-cubic (fcc) structure.[5] The A site has eightfold oxygen coordination, while the tetravalent B site has sixfold coordination. A and B sites form interpenetrating sublattices of corner-sharing tetrahedra. As the average ionic radius of the R ion r_R increases, $R_2Mo_2O_7$ undergoes a magnetic phase transition from the spin-glass insulating state to the FM metallic state.[3,4] The spin-glass phase of this series is expected from the geometrical frustration of antiferromagnetically coupled Mo spins.[6] If R ions in $R_2Mo_2O_7$ are trivalent, then Mo becomes tetravalent with two electrons accommodated in the t_{2g} orbitals of the Mo $4d$ level. A neutron diffraction study on $Nd_2Mo_2O_7$ (Refs. 7 and 8) has revealed that the FM transition below the Curie temperature $T_C \sim 90$ K is mainly due to the ordering of the Mo spins and that the saturated Mo spin moment at low temperature is $\sim 1.0\mu_B$. Unusual behavior has been observed in the anomalous Hall effect of $Nd_2Mo_2O_7$.[9] It has been proposed that the spin-polarized Mo d electrons are itinerant, whereas the Nd f electrons are localized to form the local moments in $Nd_2Mo_2O_7$, and that the spin chirality of Nd moments is transmitted to the Mo spins via the f-d exchange interaction J_{fd}.[9]

However, the electronic structures of $R_2Mo_2O_7$ have not been experimentally confirmed yet, in particular the character of Mo $4d$ electrons and the role of R $4f$ electronic states. In this paper, we have investigated the electronic structures of $R_2Mo_2O_7$ (R=Nd, Sm), using photoemission spectroscopy (PES). By using the photon energy ($h\nu$) dependence of the Mo $4d$ emission and resonant photoemission spectroscopy (RPES) near the R $4d \rightarrow 4f$ absorption edges, we have experimentally determined the partial spectral weight (PSW) distributions of Mo $4d$, O $2p$, and R $4f$ states. Experimental results are compared to band structure calculations.

II. EXPERIMENTAL AND CALCULATIONAL DETAILS

We have grown $R_2Mo_2O_7$ single crystals (R=Nd, Sm) by the floating-zone technique in an Ar atmosphere.[4] Synchrotron radiation x-ray powder diffraction measurements indicate that all the samples investigated are single phase with cubic ($Fd\bar{3}m, Z=8$) symmetry. Thermogravimetric analysis showed that the samples are stoichiometric within a resolution of 1%. PES experiments were carried out at the Ames/Montana beamline at the Synchrotron Radiation Center (SRC). Samples were fractured and measured in vacuum with a base pressure better than 3×10^{-11} Torr and at $T \lesssim 15$ K. The total instrumental resolution [full width at half maximum FWHM] was about 80 meV at $h\nu \approx 20$ eV and 300 meV at $h\nu \approx 130$–140 eV.

The linearized muffin-tin orbital (LMTO) band calculations are performed on the ferromagnetic phase of

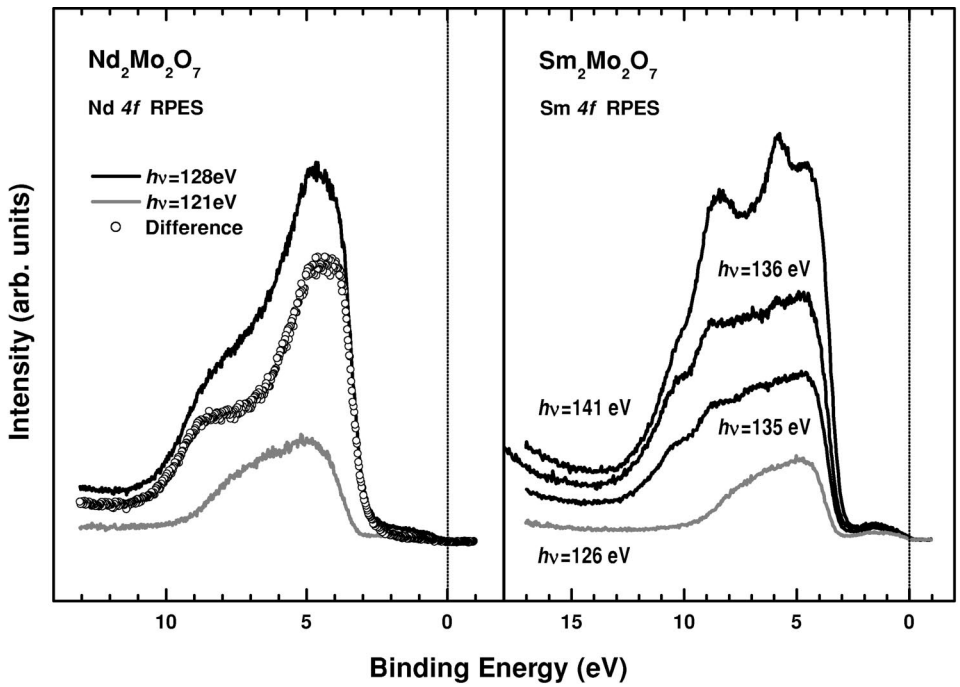

FIG. 1. Left: normalized valence-band spectra of $Nd_2Mo_2O_7$, obtained at $4d \rightarrow 4f$ on-resonance (solid line) and at off-resonance (gray line), respectively. The difference is denoted as open circles. Right: similarly for $Sm_2Mo_2O_7$. $h\nu = 136$ eV and $h\nu = 141$ eV correspond to the resonance energies of the Sm^{2+} and Sm^{3+} valence states, respectively.

$Nd_2Mo_2O_7$ with the fcc pyrochlore structure (lattice constant $a = 10.482$ Å.[4]) We have employed the local spin-density approximation (LSDA) and the LSDA+U scheme by including the effects of the on-site Coulomb correlation U between Nd $4f$ electrons and the spin-orbit (SO) interaction of Nd $4f$ electrons (LSDA+U+SO).[10]

III. RESULTS AND DISCUSSION

A. $h\nu$-dependent valence-band spectra

Figure 1 compares the normalized valence-band spectra of $Nd_2Mo_2O_7$ (left) and $Sm_2Mo_2O_7$ (right) at the on- and off-resonance energies due to the $4d \rightarrow 4f$ RPES, respectively. In $Nd_2Mo_2O_7$, $h\nu = 128$ eV and $h\nu = 121$ eV correspond to the on- and off-resonance energies, respectively. Thus the spectral features enhanced at $h\nu = 128$ eV, as compared to $h\nu = 121$ eV, can be identified as the Nd $4f$ emission, and the difference curve (dots) is considered to represent the Nd $4f$ PSW distribution. Similarly, $h\nu = 141$ eV and $h\nu = 135$ eV in $Sm_2Mo_2O_7$ correspond to the on-resonance energies of $Sm^{3+}(4f^5)$ and $Sm^{2+}(4f^6)$ valence states, respectively.[11] The off-resonance spectra of both $Nd_2Mo_2O_7$ (at $h\nu = 121$ eV) and $Sm_2Mo_2O_7$ (at $h\nu = 126$ eV) are dominated by the O $2p$ emission, and these spectra will be discussed further in Fig. 2.

The Nd $4f$ PSW shows negligible spectral intensity at E_F and consists of two large-energy-scale features, around ~ 5 eV and ~ 8 eV, respectively. These Nd $4f$ spectral features are qualitatively similar to those of other Nd oxides,[12,13] but quite different from those of Nd metal or metallic Nd compounds.[11,14] As will be explained later in Fig. 3, the Nd valence in $Nd_2Mo_2O_7$ is close to $3+$, implying that its ground state $|G\rangle$ corresponds to $|G\rangle \simeq |4f^3\rangle + \alpha_0 |4f^4 L\rangle$ (L : a ligand hole, $\alpha_0^2 \ll 1$). On the other hand, the analysis of the Nd $4f$ line shape spectrum reveals[15] that the $4f$ spectrum of $Nd_2Mo_2O_7$ cannot be explained solely by a simple $4f^3 \rightarrow 4f^2$ transition. Therefore we interpret that the Nd $4f$ PSW represents the mainly $4f^3$ ground state, but with the large final-state hybridization between Nd $4f$ and mainly O $2p$ orbitals. We assign the high- and low-binding-energy (BE) peaks in $Nd_2Mo_2O_7$ as the ionization peak ($|G\rangle \rightarrow |4f^2\rangle$) and the hybridization peak ($|G\rangle \rightarrow |4f^3 L\rangle$), respectively. These assignments are supported by the supercell Δ-SCF calculations.[16]

$Sm_2Mo_2O_7$ also exhibits the large $4f$ resonance, for which most of the resonating spectral features are observed in the 4–12 eV BE region with a very weak feature between E_F and 3 eV BE. In the PES spectra of mixed-valent Sm compounds, both the Sm^{2+} and Sm^{3+} states are observed as the $4f^5$ and $4f^4$ final-state emissions located around 3 eV BE and 5–10 eV BE regions below E_F, respectively.[11,17] Hence we assign the enhanced structures in the 6–12 eV BE region as the $4f^5 \rightarrow 4f^4$ transitions due to Sm^{3+} ions and the weak emission between 3 eV BE and E_F is as the $4f^6 \rightarrow 4f^5$ transitions due to *surface* Sm^{2+} ions.[18] The latter assignment is based on the finding in Fig. 4.

Figure 2 compares the valence-band spectra of $R_2Mo_2O_7$ (R=Nd, Sm) for $h\nu = 26$ eV (left) and at off-resonance energies of R $4d \rightarrow 4f$ RPES process (right). Here $h\nu = 26$ eV is chosen because the relative contribution from the Mo $4d$ emission is larger at $h\nu = 26$ eV than at other $h\nu$'s among our data. At $h\nu \sim 26$ eV the Mo $4d$ emission should be observable ($\sim 20\%$), even though the O $2p$ emission is still dominant ($\sim 80\%$).[19] At R $4f$ off-resonance energies, the O $2p$ emission is dominant over other electron emissions including R $4f$ emissions. Note that, when the Mo $4d$ emission is important ($h\nu = 26$ eV), the valence-band spectra of both $Nd_2Mo_2O_7$ and $Sm_2Mo_2O_7$ show an increased intensity only in the region near E_F. This behavior reflects that the

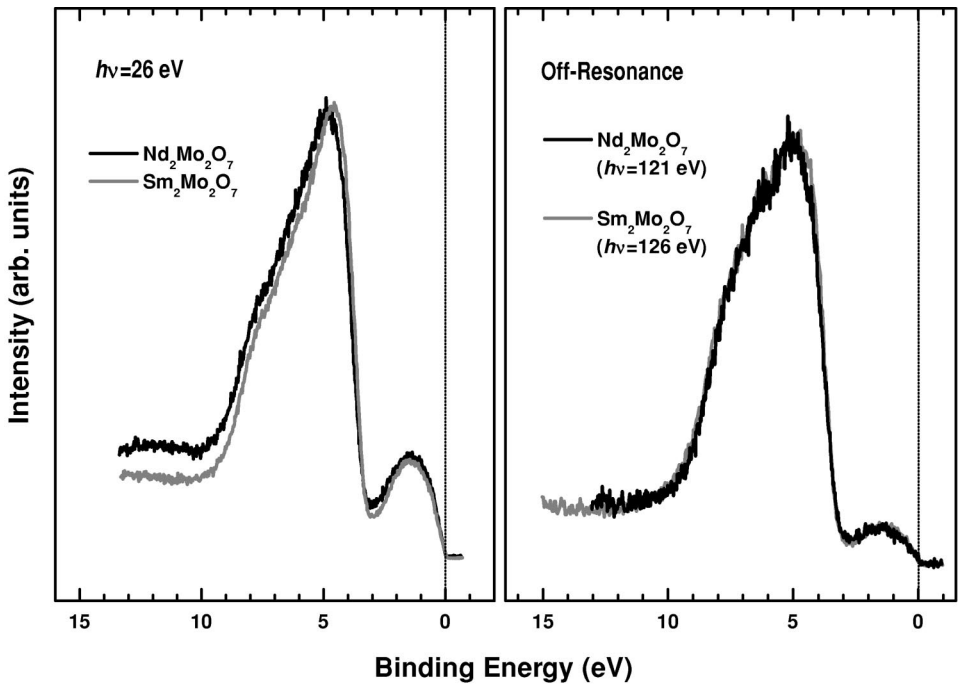

FIG. 2. Comparison of the valence-band line shapes of $R_2Mo_2O_7$ (R=Nd, Sm) at $h\nu$ =26 eV (left) and at the off-resonance energies (right).

electronic states near E_F have mainly Mo $4d$ character. Further, the overall line shapes of the valence-band spectra of $R_2Mo_2O_7$ (R=Nd, Sm) are very similar when the Mo $4d$ emission is important as well as when the O $2p$ emission is dominant. It indicates that the R $4f$ electrons do not affect much the near-E_F features of the Mo $4d$ electronic structures in $R_2Mo_2O_7$.

B. CIS and CFS spectra

Figure 3 shows the constant-final-state (CFS) partial yield spectrum and constant-initial-state (CIS) spectra of $Nd_2Mo_2O_7$ for several initial-state energies E_i's, taken across the Nd $4d\rightarrow 4f$ absorption threshold. A large enhancement at about $h\nu\sim 128$ eV in the CIS spectra reflects the Nd $4f$ resonance via the Nd $4d\rightarrow 4f$ absorption and the following Auger process with the Coulomb matrix element $\langle 4d,\epsilon_k|(1/r_{12})|4f,4f\rangle$. All the CIS spectra exhibit a Fano-type resonance in the Nd $4f$ cross section with essentially the same line shapes for different E_i values in $Nd_2Mo_2O_7$, which indicates that the electronic states in 4–10 eV BE region have a large Nd $4f$ character with essentially the same $4f$ initial-state configurations.

The CFS partial yield spectrum was taken with a kinetic energy E_K of $\sim$1.5 eV, corresponding to the electron escape depth of order of a few tens Å. Thus the spectral features in the partial yield spectra can be regarded as representing the intrinsic *bulk* spectrum of the material.[20] Indeed, the CFS corresponds to a measured photoabsorption spectrum.[21,22] The CFS yield spectrum of $Nd_2Mo_2O_7$ exhibits fine structures below the absorption threshold (around 110–122 eV) and broad giant resonances above the absorption threshold (around 124–140 eV). Both the fine structures and the giant resonance in the $4d\rightarrow 4f$ absorption arise from final-state multiplet structures with the $4d^9 4f^{n+1}$ configuration.[23] The energy separations and relative strengths among the fine structures in the absorption spectra of rare-earth compounds serve as a fingerprint for the valence state of the rare-earth ions.[22,24,25]

The inset compares the enlarged fine structures of $Nd_2Mo_2O_7$ to that of NdF_3. The latter spectrum has been reproduced from Ref. 22 and shifted so that its onset structures are aligned to those of $Nd_2Mo_2O_7$. Here NdF_3 is chosen because it is a well-known trivalent compound, with the nearly $4f^3$ electron configuration in the ground state. This comparison clearly shows that the CFS fine structures of $Nd_2Mo_2O_7$ are almost identical to those of NdF_3, providing evidence that the valence of *bulk* Nd ions in $Nd_2Mo_2O_7$ is very close to 3+.

Similarly as in Fig. 3, the Sm $4d\rightarrow 4f$ CFS partial yield spectrum and CIS spectra of $Sm_2Mo_2O_7$ are shown in Fig. 4. All the CIS spectra exhibit very similar line shapes for different E_i values except for E_i=1.5 eV. In particular, a large enhancement is observed at $h\nu\sim 141$ eV, while no pronounced enhancement is observed at $h\nu\approx 135$ eV, suggesting that *bulk* Sm ions in $Sm_2Mo_2O_7$ are mostly trivalent (3+). A slightly different CIS line shape is observed for E_i =1.5 eV, for which the maximum energy seems to occur at a lower $h\nu$ than for higher E_i values. Since $h\nu$=135 eV also corresponds to the resonance energy of the Sm^{2+} ($4f^6$) states, the CIS line shape for E_i=1.5 eV seems to suggest the existence of a small amount of Sm^{2+} ions,[18] but probably in the surface region as explained below. The inset compares the enlarged fine structures of $Sm_2Mo_2O_7$ to those of trivalent SmF_3 ($4f^5$) and divalent SmF_2 ($4f^6$).[22] The CFS fine structures of $Sm_2Mo_2O_7$ are almost identical to those of SmF_3, but are quite different from those of SmF_2, providing evidence that the amount of the divalent Sm^{2+} ions in *bulk* $Sm_2Mo_2O_7$ is negligible. Therefore it is likely that the above-mentioned Sm^{2+} contribution comes from the *surface* Sm^{2+} ions.

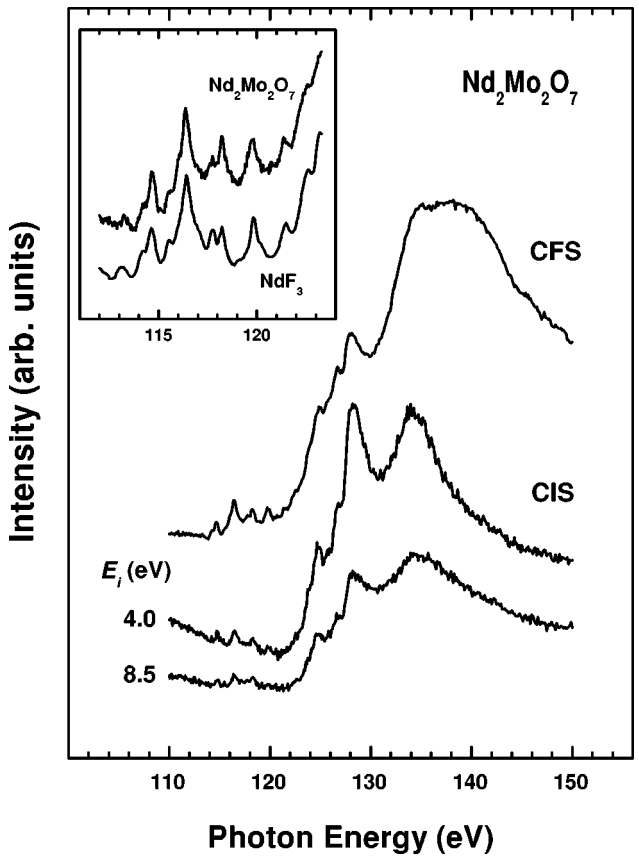

FIG. 3. Constant-initial-state (CIS) spectra of $Nd_2Mo_2O_7$ for several initial state energies E_i and the constant-final-state (CFS) partial yield spectrum (top) taken across the Nd $4d$ absorption threshold. Inset: comparison of the enlarged CFS fine structures of $Nd_2Mo_2O_7$ to those of NdF_3.

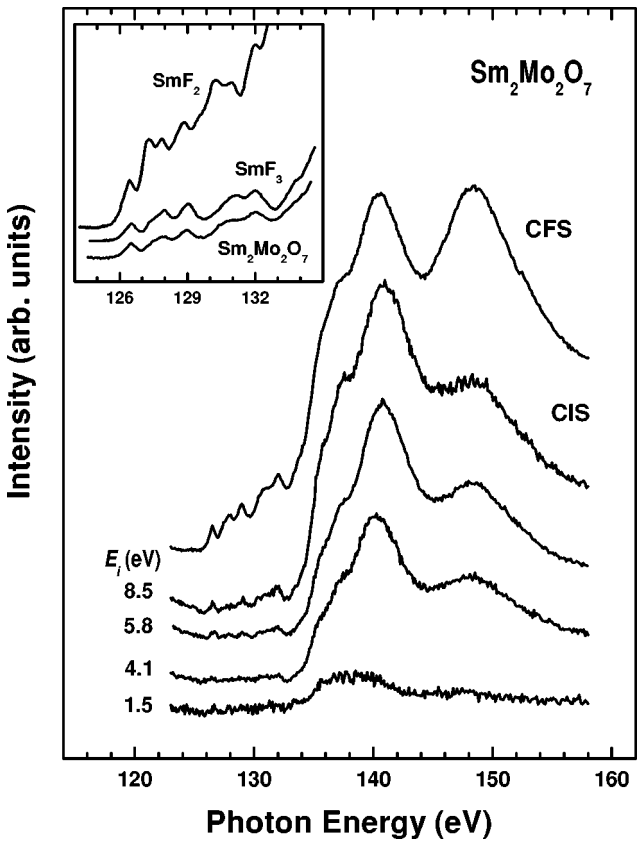

FIG. 4. CIS spectra of $Sm_2Mo_2O_7$ and the CFS partial yield spectrum (top) taken across the Sm $4d$ absorption threshold. Inset: Comparison of the enlarged CFS fine structures of $Sm_2Mo_2O_7$ to those of SmF_2 and SmF_3.

C. LSDA+U+SO electronic structure calculations

We have performed the LSDA+U+SO calculation using the Coulomb correlation parameter $U=6.0$ eV and the exchange parameter $J=0.95$ eV. The calculated Nd $5d$, Nd $4f$, Mo $4d$, and O $2p$ partial densities of states (PDOS) for $Nd_2Mo_2O_7$ are shown in Fig. 5. The upper and lower curves in each panel represent the majority-spin and minority-spin PDOS per formula unit (f.u.), respectively. There are two O types in the unit cell, and the O p PDOS in Fig. 5 corresponds to the sum of PDOSs of two O types per f.u. Due to the Coulomb correlation, the occupied Nd $4f$ states are separated from the unoccupied Nd $4f$ states and accordingly the Nd $4f$ PDOS near E_F becomes nearly zero. The spin magnetic moment of Nd is $2.7\mu_B$. The account of the spin-orbit interaction for Nd $4f$ electrons gives rise to the large orbital magnetic moment $-4.9\mu_B$. That is, the spin magnetic moment is antiferromagnetically polarized with the orbital magnetic moment, satisfying the third Hund rule, and so the total magnetic moment of Nd becomes $2.2\mu_B$. The calculated Nd $4f$ PDOS, however, does not agree well with the measured Nd $4f$ PSW (Fig. 1), suggesting that the LSDA+U+SO calculation is not enough to describe the large on-site Coulomb correlation between Nd $4f$ electrons for $Nd_2Mo_2O_7$. Consequently, the density of states near E_F is contributed mainly from the Mo t_{2g} electrons, in agreement with the experimental finding in the measured PES spectra (see Fig. 2). The calculated PDOS show a large hybridization between the Mo $4d$ and O $2p$ orbitals in $Nd_2Mo_2O_7$. It is found that Mo $4d$ bands are exchange split to yield a magnetic moment of $\sim 1.0\mu_B$ in agreement with the experiment.[7] Further, Mo $4d$ spins are antiferromagnetically polarized with Nd $4f$ spins. The calculated Mo $4d$ PDOS shows that about 3.7 d electrons are occupied. But neglecting the extended hybridized states between -8 and -4 eV, about 1.1 and 0.1 electrons are occupied in the $t_{2g}\downarrow$ and $t_{2g}\uparrow$ bands near E_F, respectively. Most interestingly, the LSDA+U+SO calculation predicts a nearly half-metallic electronic structure for $Nd_2Mo_2O_7$. The effect of this nature will be discussed below.

Figure 6 compares the measured spectra to the calculated PDOS for $Nd_2Mo_2O_7$. The left panel shows the valence-band PES spectra obtained at $h\nu=90$ eV and $h\nu=26$ eV. The $h\nu=90$ eV spectrum can be considered as the O $2p$ PSW since the Cooper minimum in the Mo $4d$ cross section occurs around $h\nu\sim 90$ eV. On the other hand, the $h\nu=26$ eV valence-band spectrum has a relatively large contribution from the Mo $4d$ electron emission. The comparison in the left panel shows that the Mo $4d$ states are located mainly between -2 eV and E_F, while the O $2p$ states are located mainly between -3 eV and -8 eV. The right

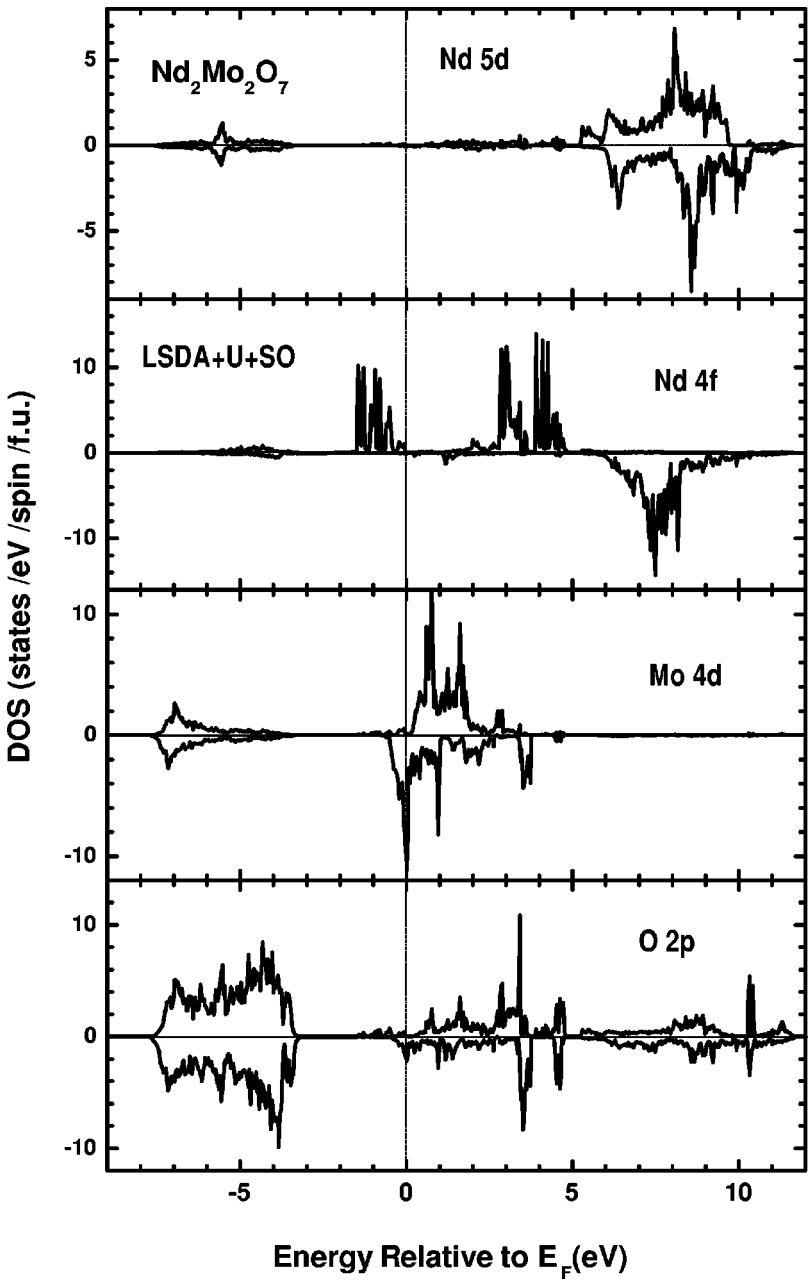

FIG. 5. The calculated partial densities of states (PDOS) for $Nd_2Mo_2O_7$, obtained from the LSDA$+U+$SO calculation. The top panel shows the majority-spin and minority-spin Nd $5d$ PDOS per formula unit (f.u.). The lower three panels show the Nd $4f$, Mo $4d$, and O $2p$ PDOS per f.u., respectively.

panel of Fig. 6 compares the weighted PDOS of the Mo $4d$, O $2p$, and Nd $5d$ states of $Nd_2Mo_2O_7$ below E_F, corresponding to the occupied part of the PDOS. The weighted PDOS are obtained by multiplying the relative photoionization cross sections for $h\nu=90$ eV and $h\nu=26$ eV, respectively,[19] to the calculated PDOS. Each theory curve is then convoluted with a Gaussian function of 0.2 eV at FWHM to simulate the instrumental resolution. The calculated electronic states near E_F have mainly Mo t_{2g} character, consistent with the experimental finding.

The trend in the measured valence-band spectra of $Nd_2Mo_2O_7$ is qualitatively consistent with that in the calculated PDOS. Nevertheless, there are also some discrepancies between experiment and theory. The calculated bandwidth of the Mo t_{2g} states below E_F ($\lesssim 1$ eV) is smaller than the width in the measured PES spectrum ($\gtrsim 2$ eV). Further, the metallic DOS obtained in the present LSDA$+U+$SO calculation does not agree with the negligible spectral weight at E_F in the measured spectra. The origin of such discrepancies is not resolved at the moment. A possible origin might be a local Jahn-Teller distortion at the Mo site or a non-negligible on-site Coulomb interaction U_{dd} between Mo $4d$ electrons.[26] These possibilities need to be checked further.

We now address the origin of the stable FM phase in $Nd_2Mo_2O_7$ pyrochlore oxides. Applying the simple Goodenough-Kanamori rule of the superexchange interaction,[27] 180° Mo-O-Mo bond would have a nearest-neighbor FM exchange via a Mo(t_{2g})-O(p_π)-Mo(t_{2g}) interaction, whereas a 90° Mo-O-Mo bond would have an antiferromagnetic (AFM) exchange. Note that this feature is opposite to the conventional sign assignment of the superexchange interaction. This is because the orbitals participating

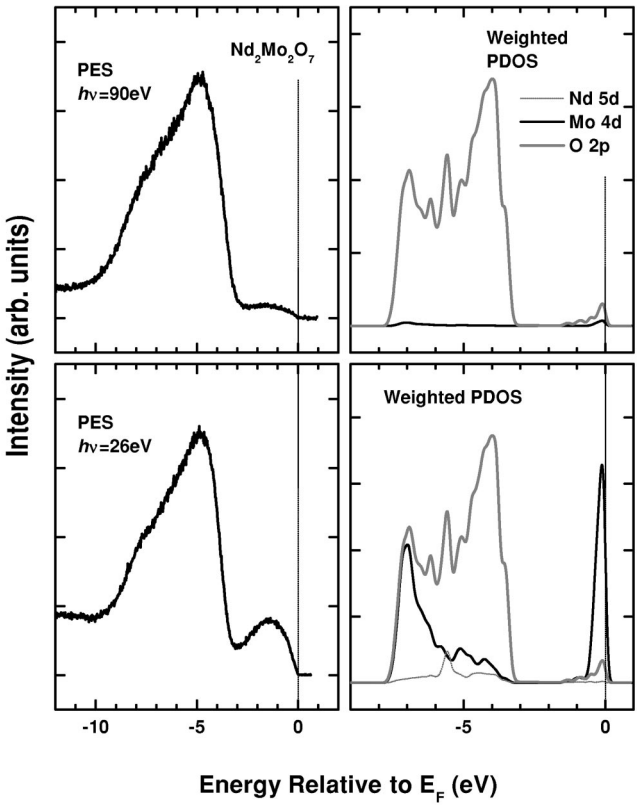

FIG. 6. Left: valence-band PES spectra of $Nd_2Mo_2O_7$ at the Cooper minimum ($h\nu=90$ eV) where the O $2p$ emission is dominant and at $h\nu=26$ eV where the Mo $4d$ emission is non-negligible. Right: the weighted PDOS of the Mo d, O p, and Nd d electrons, obtained from the LSDA$+U+$SO calculation.

in the superexchange interaction in this system are t_{2g} and p_π, since t_{2g} orbitals are not fully occupied. In the conventional case—for example, in $CaMnO_3$—the orbitals involved in the hopping of the superexchange interaction are e_g and p_σ. Since the Mo-O-Mo bond angle θ_b in $Nd_2Mo_2O_7$ is $\sim 132°$ (close to the middle of 90° and 180°),[4] the FM and AFM superexchange interactions are expected to be comparable. On the other hand, the nearly half-metallic electronic structure of $Nd_2Mo_2O_7$ (see Fig. 5) suggests that the FM interaction is favorable between Mo atoms, because then the kinetic energy gain occurs through hopping of Mo $4d$ electrons. Therefore the FM phase will be stabilized if the FM interaction, induced by the optimized kinetic energy, is dominant over the AFM superexchange interaction. The mechanism of the FM interaction in Mo pyrochlore oxides is similar to the DE interaction operating in perovskite manganites, even though the mixed-valent nature of Mo has not been clearly identified in $R_2Mo_2O_7$. The decreasing trend of T_C with decreasing r_R can be understood in the same context.[3,4] That is, with decreasing r_R, θ_b decreases to reduce the the bandwidths and the kinetic energy gain. In addition, due to the decreased θ_b, the effect of the AFM superexchange interaction becomes larger. Consequently, T_C is reduced.

IV. CONCLUSIONS

The electronic structures of $R_2Mo_2O_7$ ($R=$Nd, Sm) have been investigated using photoemission spectroscopy. The electronic states near E_F have mainly Mo $4d$ character. R $4d\rightarrow 4f$ RPES measurements ($R=$Nd, Sm) reveal that R $4f$ states are located well below E_F and that the valence of *bulk* Nd and Sm ions is very close to $3+$. The small Sm^{2+} component is also observed in the Sm $4f$ PSW of $Sm_2Mo_2O_7$, which comes from the *surface* Sm^{2+} ions. The Mo $4d$ electronic states near E_F are not affected much by R $4f$ states. The LSDA$+U+$SO band calculation indicates the nearly half-metallic electronic structure and the large hybridization between the Mo $4d$ and O $2p$ orbitals. The qualitative features of the measured valence-band spectra are described well by the LSDA$+U+$SO band structure calculation, but there are some discrepancies in the bandwidth and the spectral weight near E_F, which remain to be resolved. The stable FM phase in $Nd_2Mo_2O_7$ can be explained by the competition between the FM interaction induced by the kinetic energy optimization and the AFM superexchange interaction.

ACKNOWLEDGMENTS

This work was supported by the KOSEF through the CSCMR at SNU and the eSSC at POSTECH. The PES experiment was conducted at the SRC, University of Wisconsin–Madison, supported by the NSF Grant No. (DMR-0084402).

[1] *Electronic Conduction in Oxides*, edited by N. Tsuda, K. Nasu, A. Yanase, and K. Siratori (Springer-Verlag, New York, 1991), Chap. 1.

[2] K.-I. Kobayashi, T. Kimura, H. Sawada, K. Terakura, and Y. Tokura, Nature (London) **395**, 677 (1998).

[3] T. Katsufuji, H.Y. Hwang, and S.-W. Cheong, Phys. Rev. Lett. **84**, 1998 (2000).

[4] Y. Moritomo, Sh. Xu, A. Machida, T. Katsufuji, E. Nishibori, M. Takata, M. Sakata, and S.-W. Cheong, Phys. Rev. B **63**, 144425 (2001).

[5] M.A. Subramanian, G. Avravamudan, and G.V.S. Rao, Prog. Solid State Chem. **15**, 55 (1983).

[6] J.S. Gardner, B.D. Gailin, S.-H. Lee, X. Broholm, N.P. Raju, and J.E. Greedan, Phys. Rev. Lett. **83**, 211 (1999).

[7] Y. Yasui, Y. Kondo, M. Kanada, M. Ito, H. Harashina, M. Sato, and K. Kakurai, J. Phys. Soc. Jpn. **70**, 284 (2001).

[8] S. Yoshii, T. Iikubo, T. Kageyama, K. Oda, Y. Kondo, K. Murata, and M. Sato, J. Phys. Soc. Jpn. **69**, 3777 (2000).

[9] Y. Taguchi, Y. Oohara, H. Yoshizawa, N. Nagaosa, and Y. Tokura, Science **291**, 2573 (2001).

[10] S.K. Kwon and B.I. Min, Phys. Rev. Lett. **84**, 3970 (2000).

[11] F. Gerken, Ph.D. thesis, University of Hamburg, 1982.

[12] H. Namatame, A. Fujimori, Y. Tokura, M. Nakamura, K. Yamaguchi, A. Misu, H. Matsubara, S. Suga, H. Eisaki, T. Ito, H. Takagi,

and S. Uchida, Phys. Rev. B **41**, 7205 (1990).
[13] A. Sekiyama, S. Suga, M. Fujikawa, S. Imada, T. Iwasaki, K. Matsuda, T. Matsushita, K.V. Kaznacheyev, A. Fujimori, H. Kuwahara, and Y. Tokura, Phys. Rev. B **59**, 15 528 (1999).
[14] J.-S. Kang, J.H. Hong, D.W. Hwang, J.I. Jeong, S.D. Choi, C.J. Yang, Y.P. Lee, C.G. Olson, K.C. Kang, and B.I. Min, Phys. Rev. B **49**, 16 248 (1994).
[15] J.-S. Kang (unpublished).
[16] B.I. Min (unpublished).
[17] S. Suga, S. Imada, T. Jo, M. Taniguchi, A. Fujimori, S.-J. Oh, A. Kakizaki, T. Ishii, T. Miyahara, T. Kasuya, A. Ochiai, and T. Suzuki, Phys. Rev. B **51**, 2061 (1995).
[18] J.-S. Kang, C.J. Yang, Y.P. Lee, C.G. Olson, E.-J. Cho, S.-J. Oh, R.O. Anderson, L.Z. Liu, J.-H. Park, J.W. Allen, and W.P. Ellis, Phys. Rev. B **48**, 10 327 (1993).
[19] J.J. Yeh and I. Lindau, At. Data Nucl. Data Tables **32**, 1 (1985).
[20] In general, the L_3-edge absorption measurements are easy to show the bulk valence states of rare-earth ions. See J. Röhler, J. Magn. Magn. Mater. **47-48**, 175 (1985).
[21] D. Wieliczka, J.H. Weaver, D.W. Lynch, and C.G. Olson, Phys. Rev. B **26**, 7056 (1982).
[22] C.G. Olson and D.W. Lynch, J. Opt. Soc. Am. A **72**, 88 (1982).
[23] H. Ogasawara, A. Kotani, K. Okada, and B.T. Thole, Phys. Rev. B **43**, 854 (1991).
[24] G. Kalkowski, C. Laubschat, W.D. Brewer, E.V. Sampathkumaran, M. Domke, and G. Kaindl, Phys. Rev. B **32**, 2717 (1985).
[25] D.W. Lynch and R.D. Cowan, Phys. Rev. B **36**, 9228 (1987).
[26] A large U_{dd} between Mo $4d$ electrons might induce the shift down of the Mo t_2g bands, resulting in a larger bandwidth and reduced DOS at E_F.
[27] J. Kanamori, J. Phys. Chem. Solids **10**, 87 (1959).